Arabian Journal for Science and Engineering (2023) 48:14901–14911
https://doi.org/10.1007/s13369-023-07922-6

RESEARCH ARTICLE-ELECTRICAL ENGINEERING

A Proposed V2V Path Loss Model: Log-Ray

Kenan Kuzulugil[1] · Zeynep Hasirci Tugcu[2] · Ismail Hakki Cavdar[3]

Received: 30 July 2022 / Accepted: 30 April 2023 / Published online: 22 May 2023

Abstract
Vehicle-to-vehicle (V2V) communication that has prominent involvement in the design of innovative communication solutions for the intelligent transportation system. Therefore, to develop V2V channel models, the knowledge of the propagation channel on which comprehensive research efforts have been carried is vital. In this study, we focused on the analysis and modeling of path loss characteristics for V2V communications and proposed a log-ray path loss model with the motivation of overcoming remarkable fitting errors between the two-ray model and measured data where the path loss exponent corresponds to different from 2. First, channel measurements were performed at 5.9 GHz with commercially available DSRC OBU devices for five different scenarios in typical highway and suburban environments in Gümüşhane, Turkey. Then, the large-scale characteristics of different propagation scenarios were analyzed and the proposed log-ray model performance was compared with commonly used log-distance and two-ray path loss models qualitatively and quantitatively. On the other hand, analysis of small-scale modeling and shadowing were also conducted for all scenarios and presented in the results. The findings clearly demonstrate that the proposed log-ray path loss model fits the measured data with a smaller RMSE value (2.54 dB) than the results of the log-distance (3.07 dB) and two-ray (3.72 dB) path loss models in the literature. In other words, the proposed model has approximately 17.5% and 32% increase in fitting performance according to the log-distance and the two-ray path loss models, respectively. The study results will be helpful for better performance analysis and system design of V2V communication.

Keywords Channel measurements · Large-scale fading · Propagation model · Small-scale fading · Vehicular channels · Vehicular communications · V2V path loss models.

1 Introduction

The main idea behind vehicle-to-vehicle (V2V) communication is to prevent accidents, alleviate traffic congestion, and save more life and money. For this purpose, vehicles share data such as speed, heading, and position with other vehicles. Due to the high speed of transmitter (Tx) and receiver (Rx) vehicles, blockage by other vehicles due to lower antenna heights, and the presence of several scattering objects such as traffic lamps, lamp posts, trees, and the vehicle itself, the V2V communication channel differs from wireless communication. Thus, whether the existing communication path loss models in the literature are appropriate for the V2V communication channel in different traffic conditions, road types, and environments should be tested. Over the last decades, a considerable number of experimental studies have been carried out about V2V communication channel modeling. V2V channel modeling approaches can be discussed in the two main perspectives such as large-scale modeling and small-scale modeling. Path loss and shadowing are generally analyzed with large-scale modeling, while small-scale modeling is calculated as fast fading over the mean path loss value. In large-scale modeling, the measured data from different propagation environments are fitted to well-known path

Zeynep Hasirci Tugcu and Ismail Hakki Cavdar have contributed equally to this work.

✉ Kenan Kuzulugil
kenankuzulugil@gumushane.edu.tr

Zeynep Hasirci Tugcu
zhasirci@ktu.edu.tr

Ismail Hakki Cavdar
cavdar@ktu.edu.tr

[1] Department of Electronics and Automation, Gumushane University, 29600 Gumushane, Turkey

[2] Department of Electronics and Communications Engineering, Karadeniz Technical University, 61830 Trabzon, Trabzon, Turkey

[3] Department of Electrical and Electronics Engineering, Karadeniz Technical University, 61080 Trabzon, Trabzon, Turkey

loss models to show how a received signal power decays with the distance between Tx and Rx. Shadowing is usually modeled by a zero-mean Gaussian distribution with the standard deviation obtained from the measured data. On the other hand, small-scale modeling, also called fast fading, is modeled with well-known statistical distributions such as Weibull, Nakagami-*m*, Rayleigh, and Rician.

Experimental studies in the literature differ in terms of measurement environment, measurement setup, center frequency, antenna types, antenna positions, etc. The measurements were generally conducted in different environments such as urban [1–12], in suburban [1, 3–5, 9, 12–17], in highway [1, 3–9, 12, 18–24], in rural [3–7, 22], in forest [11] and in park [2, 25]. The measurement setups also differ from each other in these studies. Dedicated Short Range Communication On-Board Unit (DSRC OBU) kits were used in [1, 2, 9, 11–14, 19, 20, 24, 25] while a signal generator (SG) at the Tx side and a signal analyzer (SA) at the Rx side were used in [3–8, 10, 13, 15–17, 21–23]. The studies using the DSRC OBU setup can only record and analyze the received signal strength values, while the SG-SA setup can also analyze Doppler spread, delay spread, and coherence time. Additionally, if we evaluate the measurement setups in terms of antenna characteristics, antennas used in the DSRC OBU measurement system were generally omnidirectional [2–5, 7–9, 11, 17–20, 24, 25], while the SG-SA measurement setup had also MISO in [22] and MIMO in [21] antenna arrays. All measurements were performed in the center frequency range of 700 MHz to 5.9 GHz which were at 5.9 GHz in [2, 4–7, 9, 10, 12–16, 19, 20, 23, 24], at 5.8 GHz in [1, 25], at 2.85 GHz in [18], at 5.2 GHz in [3, 21], at 700 MHz in [4, 5], at 1.85 GHz in [17], at 5.75 GHz in [22], at 5.6 GHz in [8], and at 2.1 GHz in [11]. The antennas were commonly placed on the roof of the vehicles. However, to observe the effect of the antenna location, antennas were located to the bumper in [26], inside the car in [11, 17] or nearside of the vehicles in [10]. In the realm of experimental studies, measurement environments can be classified as urban, suburban, rural, highway, freeway, expressway, forest, parking lot, tunnel, and intersection. However, in this study, the measurements were performed in highway and suburban environments.

1.1 Related Works

Log-distance and two-ray path loss models are widely used in V2V communication channel modeling. Studies using the log-distance path loss model mostly present the path loss exponent (n) parameter. In the studies, two-ray path loss model is used, the ground reflection coefficient (r or Γ) or relative permittivity parameter (ϵ_r) is given. In addition, the standard deviation (σ) value is given to model the shadowing. To keep the related works section short, these values are shown in n/σ from now on. Here, n denotes the path loss exponent and σ denotes the standard deviation of the shadowing. In this literature review, V2V communication channel modeling studies were examined into two main groups: log-distance and two-ray path loss models. Additionally, these groups were also subdivided into RSSI measurements (using DSRC OBUs) and SG-SA measurements (using signal generator and signal analyzer).

There are many studies that used log-distance path loss model (hereafter called as log-distance model)([1–8, 13–23, 27–31]). In [13], RSSI measurement setup was carried out in suburban environment and n/σ values were presented as 1.57/4.2 dB; however, the SG-SA measurements were also realized in this study and obtained n/σ values were 2.32–2.75/7.1–5.5 dB. The difference between numerical results was due to the higher receiver sensitivity of SG-SA. In [1], suburban measurement was also realized and the obtained n/σ value was 1.53/3.5 dB. The authors emphasized that these discrepancies with other published results illustrate that path loss parameters were strongly dependent on the propagation environment, measurement techniques used, the physical characteristics of vehicles and the antenna heights. In [14], various measurements in which vehicles move on the same/opposite direction and the same/adjacent lane were performed in maximum 100 m Tx-Rx distance. The obtained n/σ values were 1.2–2.22/0.55–3.92 dB. The authors also proposed a new path loss model whose n value was determined as a Gaussian random variable and its value is changing between 1.6 and 1.76.

RSSI measurements of highway, freeway, open road, and expressway were analyzed collectively as the measurement conditions of these environments were nearly identical. In [2], the measurements were performed at freeway with low/moderate vehicle density and obtained n value changes between 1.99 and 2.05. RSSI power drop locations were found with a formula developed in [18], and also n value was calculated as 2.85 for the measurement data after the determination of the critical distance. In [19], the measurements were carried out on highway and n value was found as 2.4. In [1], n/σ values were 1.77/2.8 dB for highway environment. Multilink shadowing model was presented in [20], and the measurements were carried out with four different vehicles with equipped DSRC transceivers. The measurement data were separated through LOS and OLOS (obstructed-LOS) links. For NLOS links, n/σ values were obtained as 0.54–4.18/1.73–6.58 dB, while there was no n/σ results due to using two-ray model for LOS links.

In [3–5, 15–17], SG-SA measurements were performed in suburban environment and n/σ values were calculated as 1.59–3.41/2.1–6.39 dB. The antennas were placed inside the vehicles in [17] and n/σ values were 2.8–4.6/2.54–4.79 dB.

SG–SA measurements of highway, freeway, open road, and expressway environments were analyzed collectively

as the measurement conditions of these environments were nearly identical. In [3–7, 21], n/σ values were obtained as 1.33–2.78/3.1–5.94 dB. In [22], antennas were located at different locations such as on the roof, inside or rear windshields of the vehicle. According to different antenna locations, the n/σ values were calculated as 1.6–1.9/4–7.9 dB. In [8, 23], dual-slope path loss model results were presented as follows: n_1/σ_1 were 1.66–1.9/2.5–3.95 dB and $n_2/\ \sigma_2$ were 2.88–4/0.6–6.12 dB. In [27], the measurements were performed at 5.2 Ghz. The obtained n/σ values were 1.76/1.68 dB for LOS and 2.18/3.83 dB for NLOS. In [28], ray-based modeling was performed at 28 GHz and n/σ values were 1.6–2.4/1.5–3.8 dB for LOS, while 2.2–2.9/13.1–15.2 dB for NLOS. In [29], the measurements were carried out in an urban environment, but the measurement setup was not provided. The obtained n/σ values were 1.43/3.06 dB. In [30], the measurements were performed at an urban intersection of 5.2 GHz. The calculated n/σ values were 1.96/3.34 dB for LOS, while 2.64/7.8 dB for NLOS. In [31], based on ray tracing modeling, n value was calculated as 1.94 for urban straight road and 1.93 for urban intersections, respectively.

Some studies also used two-ray ground reflection path loss model (hereafter called as two-ray model) ([3, 6, 9, 10, 14, 19, 25]). In [6], the ground reflection coefficient (r) and σ were calculated as 0.264 and 2.7 dB for rural environment, while 0.353 and 2.3 dB for highway environment, respectively. In [3], r/σ values were given as 0.44/2.6 dB. In [19] and [25], two-ray model was used to compare fitting results with other models, but any corresponding parameter value was not presented in these studies. In [9], an RSSI measurement system was used, and measurements were carried out on a highway, urban, suburban, and open area. To model measurement data, free-space path loss model and two-ray model were used and the authors argued that modified two-ray model fits better than free space in most cases. The relative permittivity (ϵ_r) value was given as 1.003 to calculate effective ground reflection coefficient. Also, σ value was obtained between 3.3 dB and 5.7 dB. In [10], SG-SA measurement setup was used and the ground reflection coefficient was calculated as 0.7 by tuning to match the measurement data. In [14], the relative permittivity value was chosen as 3.75 for calculations.

In this study, a path loss model named log-ray is proposed. The motivation of this proposal is to overcome the fitting errors between the two-ray model and the measured data by taking into account the nature of V2V propagation environments and also to provide better representations in terms of large-scale modeling.

The remainder of the study is organized as follows. Section 2 describes the V2V channel modeling approaches, including path loss, shadowing, and multipath. Section 3 presents the measurements campaigns which contain experimental setup, environments, and scenarios. Section 4 is devoted to the proposed log-ray path loss model. The path loss model comparisons as quantitatively and qualitatively are given in Sect. 5. Finally, Sect. 6 concludes the paper with a summary of the observations and outcomes.

2 V2V Communication Channel Modeling

V2V communication channel can be divided into two parts: large-scale fading and small-scale fading. Large-scale fading includes distance-dependent path loss and shadowing. Small-scale fading is generally determined as fast fluctuations over mean path loss. Shadowing occurs due to the communication passed through objects such as buildings, trees, and vehicles between the transmitter and the receiver. Small-scale fading consists of multipath caused by propagation mechanisms of reflection, diffraction, and scattering. Reflection occurs from large-scale objects such as buildings; diffraction occurs from a sharp corner of large-scale objects such as mountains and buildings; and scattering arises from small-scale objects such as trees, traffic lamps, and traffic signs. In this study, the received signal strength is divided into three parts: path loss, shadowing, and multipath. Then, each part is modeled one by one and all models are combined to obtain the most suitable V2V channel model.

2.1 Path Loss Modeling

The path loss, which represents signal attenuation as a positive quantity measured in dB, is defined as the difference (in dB) between the effective transmitted power and the received power [32]. Path loss highly depends on the environment (to even scenarios) of V2V communication measurements performed. Therefore, different channel models are convenient for each environment or scenario. In this study, the log-distance path loss model and the two-ray ground reflection path loss model, which are the most used path loss models in V2V communication, are used.

2.1.1 Log-Distance Path Loss Model

Both theoretical and measurement-based propagation models indicate that average received signal power decreases logarithmically with distance, whether in outdoor or indoor radio channels. Such models have been used extensively in the literature. The average large-scale path loss for an arbitrary Tx–Rx separation is expressed as a function of distance by using a path loss exponent, n;

$$\mathrm{PL}(d) = \mathrm{PL}_{d0} + 10n\log(d/d_0) \tag{1}$$

where n is the path loss exponent which indicates the rate at which the path loss increases with distance, d_0 is the close-in reference distance which is determined from measurements

close to the transmitter, PL_{d0} is the path loss at the reference distance, and d is the Tx-Rx separation distance [32]. n value changes between 2 and 5 for classical wireless communication and is equal to 2 for free-space environment. However, n is calculated lower than 2 in many V2V measurements studies and rarely higher than 5 for density building and forest environments [11]. The most important part of calculating n using (1) is to first determine optimum d_0 value from the measurement data. The d_0 value is typically chosen a fixed value such as 1 m or 10 m in many measurement studies. This may cause deviation on calculating the best-fitted n. In [24], we proposed an approach related to this problem to find optimum d_0, PL_{d0} and best-fitted n based on the measurement data. According to this approach, the d_0 is chosen as minimum distance value in the measurement data. Then, the mean PL_{d0} value corresponding to the chosen d_0 value is also calculated from the measurement data. n value is calculated by using least-square method after substituting chosen d_0 and PL_{d0} values into (1). Afterward, the second distance value and corresponding mean path loss value are chosen as new d_0 and PL_{d0} values, respectively. The calculation process of n value is repeated for new d_0 and PL_{d0} values, and another n value is obtained. This process is repeated for all distance values up to 100 m (because, reference distance should be closer to transmitter as much as possible [32]). The new log-distance path loss models are generated by substituting d_0, PL_{d0}, and n values into (1). Then, the errors between the generated models and the measurement data are calculated. The n value with minimum error is determined as n_{best} value, and the d_0 value used to generate n_{best} is chosen as optimum reference distance. In this study, n values were obtained from (1) using this described approach in [24].

2.1.2 Two-Ray Path Loss Model

Power law models, such as log-distance model, take into account only one path, which is a non-obstructed line-of-sight (LOS) ray, between the Tx and Rx. Two-ray ground reflection path loss model consists of both direct path (LOS) and ground-reflected path. The formulation of two-ray model is given as follows [32]:

$$E_{\text{tot}}(d,t) = \frac{E_0 d_0}{d_{\text{direct}}} cos\left(\omega_c\left(t - \frac{d_{\text{direct}}}{c}\right)\right) + \Gamma\frac{E_0 d_0}{d_{\text{refl}}}\cos\left(\omega_c\left(t - \frac{d_{\text{refl}}}{c}\right)\right) \tag{2}$$

where E_0 is the free-space E-field (in units of V/m) at a reference distance (d_0) from the transmitter, ω_c is the carrier frequency in radians per second, d_{direct} is the distance of the direct path between Tx and Rx, t is the time in second, c is the speed of light given in m/s, Γ is the ground reflection coefficient, and d_{refl} is the distance of the ground-reflected path between Tx and Rx.

The simplified two-ray model has been used in most studies. This model assumes that $d \gg h_t + h_r$ while calculating ground reflection coefficient (Γ) and distance d_{refl}. However, using the actual height of the antennas is important. Because even small differences in height of either Tx or Rx result in a significantly different interference relationship between the direct and ground-reflected ray. This is also emphasized and used in [12]. For the case when the first medium is free space, the reflection coefficients for the two cases of vertical and horizontal polarization can be simplified to [32]

$$\Gamma_{\parallel} = \frac{-\epsilon_r \sin\theta_i + \sqrt{\epsilon_r - \cos^2\theta_i}}{\epsilon_r \sin\theta_i + \sqrt{\epsilon_r - \cos^2\theta_i}} \tag{3}$$

$$\Gamma_{\perp} = \frac{\sin\theta_i - \sqrt{\epsilon_r - \cos^2\theta_i}}{\sin\theta_i + \sqrt{\epsilon_r - \cos^2\theta_i}} \tag{4}$$

where ϵ_r is the relative permittivity and θ_i is the incident angle. The relative permittivity is not chosen at a fixed value (1.003 or 3.75) as in [12, 14]. The antenna location, diffraction over the vehicle roof, and the roughness of the road affect the reflection coefficient. Therefore, in this study, ϵ_r values were calculated using least-square method to minimize error between the two-ray model and the measurement data for each different scenarios.

2.2 Shadowing

The multipath in the raw measurement data should be removed to analyze shadowing. For this purpose, the average of signal strength received should be calculated in a determined interval which was chosen 3 m distance. Because, it should be greater than GPS sensitivity (2.5 m) and have enough data points in statistical evaluation. Thus, the multipath effect was removed from the data. After that, remaining data include both path loss and shadowing components. Finally, the shadowing part was obtained after removing the path loss component modeled by log-distance or two-ray according to better fitting performance from the remaining data. Shadowing is generally modeled with zero-mean Gaussian distribution in V2V communication ([1, 3, 7, 8, 13–16]) and presented with the standard deviation (σ) of this Gaussian distribution calculated from the shadowing part.

2.3 Multipath

Multipath in the radio channel creates small-scale fading effects and assumes rapid fluctuations over the average signal power received in measurement data. After the average received signal strength is removed from the raw data, the multipath part remains. This process is carried out by using

a sliding window of determined distance interval (three meters). However, the received signal values corresponding to the same distance at different moments are handled together when the measurement data are analyzed based on the distance. In other words, the multipath effect belongs to different times corresponding to the same distance can be evaluated. This causes multipath to be interpreted incorrectly. Therefore, path loss deviations is interpreted as multipath when an analysis is made depending on sliding window of distance. To overcome this problem, the measurement data are evaluated according to the time, not distance. The multipath is analyzed according to the order of the packet sequences to make an evaluation in terms of time. In the literature, the multipath is modeled with commonly used statistical distributions such as Rician, Weibull, Nakagami-*m*, and Rayleigh and Akaike Information Criteria (AIC) is used in selecting the most suitable model ([25]). AIC is calculated as

$$AIC = n\left[\ln\left(\frac{\mathrm{RSS}}{n}\right)\right] + 2k \tag{5}$$

when using residual sum of squares (RSS). k is the number of parameters in the model, and n is the sample size [33]. The smallest value of AIC indicates the best model for the data. However, the best model among of the candidate models is chosen with Akaike weights whose formula is as follows:

$$\omega_i = \frac{e^{-0.5\Delta_i}}{\sum_{r=1}^{R} e^{-0.5\Delta_r}} \tag{6}$$

Here, $\Delta_i = AIC_i - \min(AIC)$. Akaike weight is between 0 and 1. Sum of all Akaike weights is equal to 1. The model with the highest Akaike weight is considered the most suitable model for the multipath.

3 Measurement Campaigns

3.1 Measurement Setup

Two vehicles (2015 Ford Focus, 2004 Volkswagen Bora) which have almost similar heights were used for V2V communication channel measurements. The measurement setup in both vehicles includes a DSRC OBU (with GPS and DSRC antennas), a laptop, a car camera, a 12/220 V inverter, and a car cigarette lighter splitter as shown in Fig. 1. The specifications of DSRC OBU used in this study are summarized in Table 1. Two omnidirectional DSRC antennas connected to DSRC OBUs were mounted on the roofs of the vehicles. The car cameras were used to analyze the measurements as needed. For the measurements, laptops send commands to DSRC OBU via Ethernet port to generally start/stop the records. The car cigarette lighter splitters were used to multiply the car cigarette lighter that supplies all devices. The inverters were used to charge the laptops.

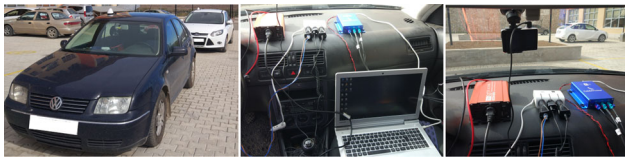

Fig. 1 Measurement setup

Table 1 DSRC OBU specifications

Parameter	Values
Standard	IEEE 802.11p
Center frequency	5.9 GHz
Data rate	3–27 Mbps
Transmitted power	22 dBm
Antenna gain	5 dBi
Antenna heights	Vehicles - 1.48 m (Tx) and 1.45 m (Rx) + 0.1 m antenna heights
Receiver sensitivity	−99 dBm at 3 Mbps

3.2 Measurement Environments and Scenarios

V2V communication measurements were carried out in highway and suburban environments in Gümüşhane, Turkey, as shown in Fig. 2. In total, 112859 data packets were collected during the measurements. Highway (H) is two-lane roads in each direction with low traffic density and vehicles driving at high speeds. Suburban (SU) is a two-lane roads in each direction (separated by median strip) with medium traffic density and vehicles moving at medium speeds. In addition, the latitude and the longitude coordinates of the measurement environments are given in terms of decimal degrees in the caption of Fig. 2.

4 Proposed Model

Log-distance and two-ray models are widely used in V2V communication path loss modeling. In this study, first, the raw data (in Fig. 3a) obtained from a highway environment were modeled with these two models as shown in Fig. 3b. Then, one that has the highest R^2 value between measurement data and model results was defined as a selection criterion in order to determine the most suitable one among the two aforementioned propagation models. However, some shifting errors occur when the measurement data are fitted to one of these models. For instance, in Fig. 3b, although the two-ray

(a) Highgway (H - 40.104328, 39.459137)

(b) Suburban (SU - 40.115951, 39.447719)

Fig. 2 Measurement environments

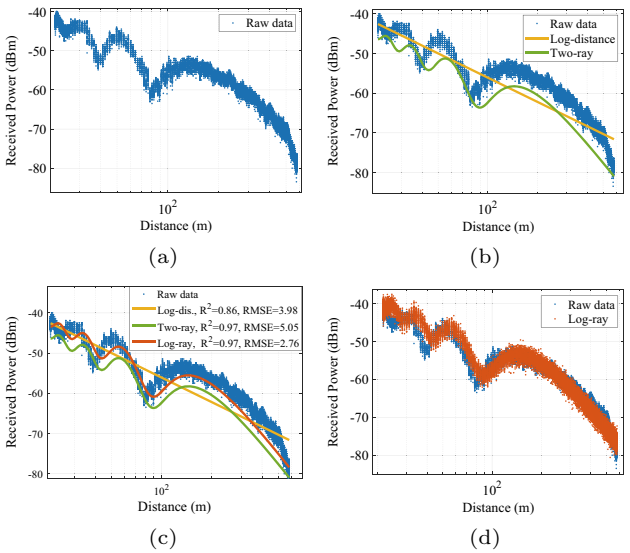

Fig. 3 An example of path loss modeling. Blue dots show the raw data, yellow line shows the log-distance model, green line shows the two-ray model, and orange line/dots show the best-fitted path loss model (log-ray)

model has the highest R^2 value, there is a non-negligible shift between the model and the measurement data. Thus, another selection criterion should also be defined for a better path loss modeling. In our study, the RMSE value between the measurement data and model was preferred as a selection criterion in addition to the R^2 value to increase the modeling performance.

On the other hand, although the combination of R^2 and RMSE values provides better modeling performance, there is still a considerable shift in some data modeled with two-ray path loss, as in Fig. 3b. The reason for this is that the parameter variation in the two-ray path loss modeling is limited only by the ratio of the constructive and destructive effect of the ray reflected from the ground. In other words, the direct ray value of the two-ray path loss model corresponds to the log-distance model whose n parameter is 2 (as in free space). However, the n value can be less or more than 2 in V2V communication. Therefore, even if the measurement data characteristically follow the two-ray model, shifts occur between the two-ray model and the data when n is different from 2. To correct this shift error due to the constant n=2 value, the model parameters should be both sensitive to the path loss exponent changing and represented by characteristics of the two-ray model. In this study, to overcome the representation problems of the raw data, a new modified model named "Log-Ray Path Loss Model" (hereafter called as log-ray model) is proposed by combining the log-distance and two-ray models. In Fig. 3c, the comparison of log-distance, two-ray, and log-ray models in terms of fitting performance is presented. It is clearly seen that log-ray model fits the measured data better than the other models. Finally, the combination of the most suitable shadowing, multipath, and best-fitted proposed model (log-ray) is obtained in Fig. 3d. The following equations are provided to clarify how log-ray model is achieved theoretically.

The received power at distance d from the Tx, $P_r(d)$, according to the Friis free-space loss equation is given as

$$P_{\mathrm{r}}(d) = \frac{P_t G_t G_r \lambda^2}{(4\pi)^2 d^2} \tag{7}$$

where P_{t} is the transmitted power (W) from the Tx, λ is the wavelength (m), Gt and Gr are Tx and Rx antenna gains, respectively. The free-space received power $P_{\mathrm{r}}(d)$ (W) can be given with the power flux-density (P_{d}) and effective antenna aperture (A_e) as

$$P_{\mathrm{r}}(d) = P_d A_e = \frac{|E(d,t)|^2}{120\pi}\frac{G_{\mathrm{r}}\lambda^2}{4\pi} = \frac{|E(d,t)|^2 G_{\mathrm{r}}\lambda^2}{480\pi^2} \tag{8}$$

where $E(d,t)$ is the free-space electric field at the distance d and given as

$$E(d,t) = \frac{E_0 d_0}{d}\cos\left(\omega_c\left(t - \frac{d}{c}\right)\right) \tag{9}$$

where E_0 is the electric field at the reference distance d_0 from the at Tx. In (8), $|E(d,t)|$ represents the envelope of the electric field at a distance d and equals $E_0 d_0/d$. Thus, the square of the electric field amplitude in (9) can be written as

$$|E(d,t)|^2 = E_0^2\left(\frac{d_0}{d}\right)^2 \tag{10}$$

where $(d_0/d)^2$ indicates the variation of the electric field with the square of the distance, and this square expression comes from the path loss exponent for free space n= 2. In the log-ray model, by using the n value obtained from the measurements instead of the square expression in (10), the electric field at the Rx is obtained that represents the characteristics of the propagation environments that differ from free-space conditions. Thus, the expressions $|E(d,t)|^2$ and $|E(d,t)|$ are rearranged as

$$|E(d,t)|^2 = E_0^2 \left(\frac{d_0}{d}\right)^{n=2} \tag{11}$$

$$|E(d,t)| = E_0 \left(\frac{d_0}{d}\right)^{n/2} \tag{12}$$

By this way, $E_{log-ray}(d,t)$, the total electric field at Rx of the proposed log-ray model can be obtained with substituting (12) in (2) as

$$E_{\text{log-ray}}(d,t) = E_0 \left(\frac{d_0}{d'}\right)^{n/2} \cos\left(\omega_c \left(t - \frac{d'}{c}\right)\right) + \Gamma E_0 \left(\frac{d_0}{d''}\right)^{n/2} \cos\left(\omega_c \left(t - \frac{d''}{c}\right)\right) \tag{13}$$

Finally, the received signal power in the proposed log-ray model, $P_{\text{log-ray}}(d)$, at the distance d can be calculated as

$$P_{log-ray}(d) = \frac{|E_{\text{log-ray}}|^2 G_r \lambda^2}{480\pi^2} \tag{14}$$

In order to use the log-ray model, firstly, n, d_0 and PL_{d0} values should be obtained for the related propagation environment [24]. Then, the received signal power corresponding to the optimum reference distance, $P_r(d_0)$, can be calculated as $P_r(d_0) = P_t - PL_{d_0}$ and E_0 is obtained as

$$E_0 = \sqrt{\frac{P_r(d_0)480\pi^2}{G_r\lambda^2}} \tag{15}$$

Lastly, after obtaining the values of n, d_0 and E_0, the total electric field, $E_{\text{log-ray}}(d,t)$, and the received signal power, $P_{\text{log-ray}}(d)$, for the proposed log-ray model are calculated according to (13) and (14), respectively.

5 Results

A path loss modeling based on five different measurement scenarios at 5.9 GHz was carried out in highway and suburban environments were presented in this paper. These scenarios can be classified as highway same direction (Hs) where the measured vehicles move in the same direction, highway low/high speed (Hls/Hhs) where the measured vehicles move at slow and high speed, and suburban same/opposite direction (SUs/SUo) where the measured vehicles move in the same or opposite direction. All the simulations were conducted in MATLAB® environment.

First, path loss parameters (n, d_0, and PL_{d0}) were calculated by using the authors' previously proposed approach [24] which is based on optimum d_0 estimation and best n calculation according to the nature of measured data. Obtained n, d_0, PL_{d0}, and ϵ_r for five different scenarios in highway and suburban environments are given in Table 2. In this study, n values of 1.5–1.81 in highway scenarios and 1.71–1.92 in suburban scenarios were obtained, while ϵ_r values were calculated between 1.007 and 1.014 in highway scenarios and between 1.005 and 1.006 in suburban scenarios. The n values obtained for LOS, NLOS, and OLOS links in highway, freeway, open road, and expressway environments from similar RSSI and SG-SA measurements in the literature were 1.77 in [1], 1.99–2.05 in [2], 1.33–2.78 in [3–7] and [21], 2.4 in [19], and 1.6–1.9 in [22]; the n values obtained in the suburban environment are 1.57 in [1], 1.59–3.41 in [3–5] and [15–17], 1.57 in [13], 1.2–2.22 and 1.6–1.76 in [14]. In this context, it has been seen that the obtained n values are in agreement with other results in the V2V literature. If an evaluation is made in terms of ϵ_r values, few studies have presented ϵ_r values, directly. In [9], this value was found to be 1.003, which is consistent with our study. On the other hand, in [19, 25], although two-ray was used for path loss modeling, no ϵ_r value result was reported. In [3], [6], and [10], r values were obtained instead of ϵ_r values and were given as 0.44, 0.353, and 0.7, respectively. Then, the large-scale characteristics of different propagation scenarios were analyzed with path loss modeling. Visual comparisons of path loss modeling were conducted for five different measurement scenarios, as shown in Fig. 4. These qualitative results were given to compare the performance of the proposed log-ray model over the other two models (log-distance and two-ray) in Fig. 4a, c, e, g, i. One can conclude from Fig. 4 that although the two-ray model seems to be one of the appropriate models to represent measured data, the results of the log-ray model provide a better modeling performance by overcoming the unrecoverable shifting errors. Last, in Fig. 4b, d, f, h, j, a comparison of the log-ray Model with measured data was shown with the combination of the most appropriate shadowing and multipath model.

Additionally, the quantitative results for all path loss models and propagation scenarios are given in Table 2 for a complete comparison. These values show the metrics of R^2 and RMSE of measurement data and model results for highway and suburban environments. If a comparison is made in terms of the R^2 criterion (in Table 2), while the average R^2 value in five different propagation scenarios was calculated as approximately 0.92 for two-ray and log-ray models, it was

Table 2 Comparison of the proposed log-ray model with other path loss models

Scenarios	Path loss parameters				R^2			RMSE (dB)			Multipath	Shadowing (dB)	Data size (packets)
	n	d_0	PL_{d0}	ϵ_r	log dist.	Two-ray	log-ray	log dist.	Two-ray	log-ray			
Hs	1.81	24.59	70.29	1.007	0.88	0.97	0.97	3.21	5.62	2.01	Nakagami-m	0.54	17212
Hls	1.50	9.20	67.48	1.012	0.85	0.91	0.89	2.71	3.19	2.50	Nakagami-m	1.21	27413
Hhs	1.61	10.68	67.38	1.014	0.90	0.95	0.94	2.58	2.66	2.24	Rician	0.89	12562
SUs	1.71	60.72	77.85	1.005	0.82	0.88	0.88	3.54	3.85	3.14	Rician	1.39	30627
SUo	1.92	65.95	78.05	1.006	0.85	0.92	0.92	3.35	3.30	2.83	Rician	1.02	25045

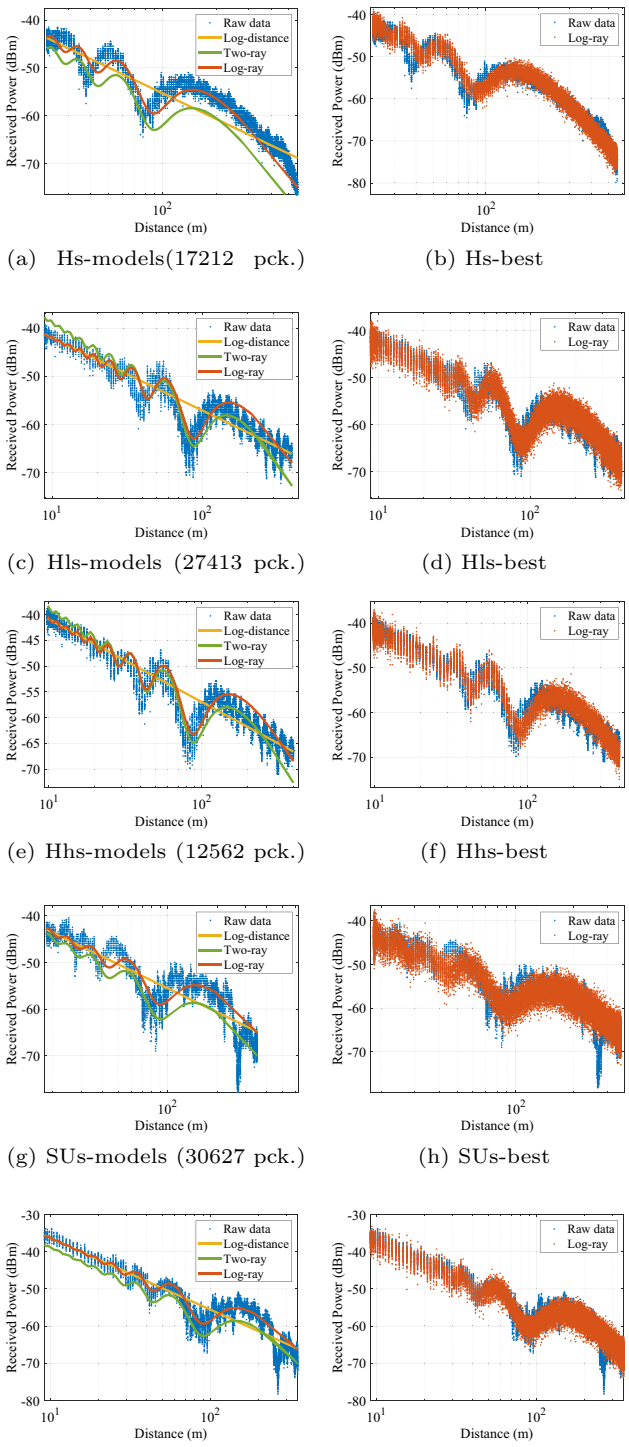

(a) Hs-models(17212 pck.) (b) Hs-best

(c) Hls-models (27413 pck.) (d) Hls-best

(e) Hhs-models (12562 pck.) (f) Hhs-best

(g) SUs-models (30627 pck.) (h) SUs-best

(i) SUo-models (25045 pck.) (j) SUo-best

Fig. 4 Log-ray path loss model results. The letters in the figures are abbreviations for H: highway, SU: suburban, s: same direction, o: opposite direction, ls: low speed, hs: high speed, and pck:packets

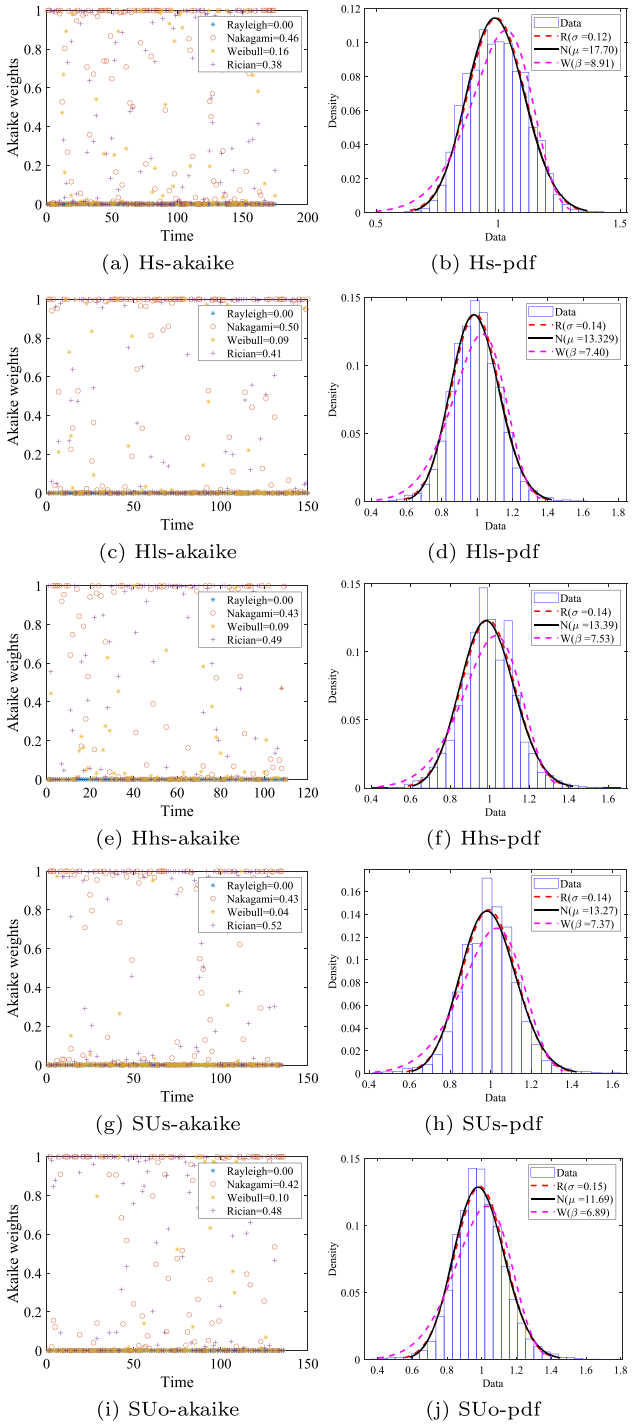

Fig. 5 Akaike and probability density function (pdf) results of multipath models of the measurement scenarios in Table 2. The abbreviations are R: Rician, N: Nakagami, and W: Weibull distributions. The values in parentheses are the parameters of the models

calculated as 0.86 for the log-distance model. In other words, the model with the worst fit was the log-distance. However, as we mentioned in Fig. 3 before, it is not enough to choose only the one with a high R^2 value when determining the most suitable model. Thus, not only a higher R^2 value but also a lower RMSE value should be the criteria for determining the best-fit model. When the log-ray and two-ray models have the highest R^2 values, it is clearly seen that for the Hs, Hls, Hhs, SUs, and SUo scenarios, the RMSE values of 5.62 dB, 3.19 dB, 2.66 dB, 3.85 dB, and 3.30 dB in two-ray changed as 2.01 dB, 2.50 dB, 2.24 dB, 3.14 dB, and 2.83 dB in the log-ray model, respectively. That is, the fitting errors of the proposed model decreased by 64%, 21%, 15%, 18.4%, and 14% compared to the two-ray model for the Hs, Hls, Hhs, SUs, and SUo scenarios, respectively. As a result, it is clearly seen that the log-ray model has the smallest fitting errors for all propagation conditions.

On the other hand, small-scale characteristics of the five different propagation scenarios were analyzed with statistical distributions such as Rician, Weibull, Nakagami-*m*, and Rayleigh. For all the calculations, the data points were grouped and analyzed at intervals of 3 m over time. First, the probability distribution functions (PDFs) of the measured data and candidate statistical models were obtained as shown in Fig. 5b, d, f, h, and j. Then, the AIC which evaluates the goodness-of-fit between the statistical models and measured data was used in the most suitable model selection as preferred in [25]. Figure 5a, d, f, h, j shows a plot of the Akaike weights calculated by (5) and (6) for the statistical distributions that have been widely used in the V2V scenarios. After multipath modeling, several observations in this comparison (in Fig. 5) are worth noting. Nakagami-m distribution shows the best fit in the Hs and Hls scenarios for 46% and 50%, respectively, while the Rician distribution also indicates a reasonable fit with a best-fit rate of 38% and 41%. Additionally, the Rician distribution has the best-fit rate of 49%, 52%, and 48% in the Hhs, SUs, and SUo scenarios, respectively, while the Nakagami-m distribution also shows a reasonable fit with a best-fit rate of 43%, 43%, and 42%. As a result, we concluded that Nakagami-m and Rician distributions are generally good at representing each scenario, while Weibull and Rayleigh distributions do not provide the best fit in five V2V scenarios as shown in Fig. 5. Nakagami-m distribution offered the perfect for Hs and Hls scenarios, while Rician distribution performed best for Hhs, SUs, and SUo scenarios as presented in Table 2. Finally, shadowing was modeled with a zero-mean Gaussian distribution, and the results were obtained as given in Table 2 for five different propagation scenarios. The standard deviation of Gaussian distribution is related to the propagation environment and was calculated from the measured data as 0.54 dB, 1.21 dB, 0.89 dB, 1.39 dB, and 1.02 dB for Hs, Hls, Hhs, SUs, and SUo, respectively.

6 Conclusion

In this study, the log-ray path loss model has been proposed for large-scale modeling of V2V communication channels taking into account the changing n value due to the nature of propagation environments. The main motivation of this work is to overcome the fitting errors between the two-ray model and the data when n is especially different from 2 and furthermore to provide a more realistic representation of the measured data with a modified path loss model including the changing n parameter. The extensive sets of measurement data were collected mainly in two propagation environments (highway and suburban) for five different scenarios. The fitting performances were compared with R^2 and RMSE as quantitatively (in Table 2) and were compared qualitatively (in Fig. 4) for all scenarios. The average RMSE value of the log-ray model in five different propagation scenarios is 2.54 dB, which is 17.5% and 32% better than the log-distance and two-ray models, which are 3.07 dB and 3.72 dB, respectively. These results prove that our proposed log-ray model fits the measured data better than both log-distance and two-ray models.

On the other hand, small-scale modeling and shadowing were also analyzed for all measured data because other vehicles, roadside trees, etc., can lead to channel fading, and the fading varied with the propagation environment. For the sake of completeness, small-scale and shadowing modeling results were also combined with the log-ray model to show the most suitable V2V channel model. The multipath was modeled best with Nakagami-m and Rician statistical distributions, and AIC was selected as the decision criterion since it is frequently used in the literature (Fig. 5). As a result, it is clearly seen that the proposed log-ray modeling presents more accurate representations as shown in Table 2. In this aspect, to the best of the authors' knowledge, the log-ray path loss modeling approach is proposed for the first time for V2V channel modeling. We believe that the proposed model will be very helpful for path loss investigations based on V2V communication channel measurements and additionally can serve as the basis for the design of V2V communication systems. In the future, more data for different propagation environments in Turkey such as urban, suburban, rural, highway, freeway, expressway, forest, parking, and tunnel can be measured. Thus, overall, the proposed log-ray model performance can be compared with existing path loss modeling approaches in the literature to contribute to the further V2V channel modeling studies.

Acknowledgements This work was supported by the Scientific Research Projects Coordination Unit of Karadeniz Technical University. Project number: 7350.

References

1. Onubogu, O.; Ziri-Castro, K.; Jayalath, D.; Ansari, K.; Suzuki, H.: "Empirical vehicle-to-vehicle pathloss modeling in highway, suburban and urban environments at 5.8 GHz". In: 2014, 8th International Conference on Signal Processing and Communication Systems, ICSPCS 2014 - Proceedings, pp. 7–12, (2014)
2. Kukshya, V.; Krishnan, H.: Experimental measurements and modeling for Vehicle-to-Vehicle Dedicated Short Range Communication (DSRC) wireless channels. In: IEEE Vehicular Technology Conference, pp. 223–227, (2006)
3. Karedal, J.; Czink, N.; Paier, A.; Tufvesson, F.; Molisch, A.F.: Path loss modeling for vehicle-to-vehicle communications. IEEE Trans. Veh. Technol. **60**(1), 323–328 (2011)
4. Fernandez, H.; Rubio, L.; Rodrigo-Penarrocha, V.M.; Reig, J.: Path loss characterization for vehicular communications at 700 MHz and 5.9 GHz under LOS and NLOS conditions. IEEE Antennas Wirel. Propag. Lett. **13**, 931–934 (2014)
5. Rubio, L.; Rodrigo-Penarrocha, V. M.; Reig, J.; Fernandez, H.: Investigation of the path loss propagation for V2V communications in the opposite direction. In: 2016 IEEE Antennas and Propagation Society International Symposium, APSURSI 2016 - Proceedings, pp. 1685–1686, (2016)
6. Kunisch, J.; Pamp, J.: Wideband car-to-car radio channel measurements and model at 5.9 GHz. In: IEEE Vehicular Technology Conference, pp. 1–5, (2008)
7. Fernández, H.; Rubio, L.; Reig, J.; Rodrigo-Peñarrocha, V.M.; Valero, A.: Path loss modeling for vehicular system performance and communication protocols evaluation. Mobile Netw. Appl. **18**(6), 755–765 (2013)
8. Abbas, T.; Sjöberg, K.; Karedal, J.; Tufvesson, F.: A measurement based shadow fading model for vehicle-to-vehicle network simulations. Int. J. Antennas Propag. **2015**, 1–12 (2015)
9. Boban, M.; Viriyasitavat, W.; Tonguz, O.: Modeling vehicle-to-vehicle line of sight channels and its impact on application-layer performance. In: VANET 2013 - Proceedings of the 10th ACM International Workshop on VehiculAr Inter-NETworking, Systems, and Applications, pp. 91–93, (2013)
10. Karlsson, K.; Carlsson, J.; Olbäck, M.; Vukusic, T.; Whiton, R.; Wickström, S.; Rogö, J.: Utilizing two-ray interference in vehicle-to-vehicle communications", , no. EuCAP, pp. 2544–2547, (2014)
11. Ibdah, Yazan; Ding, Yanwu; et al.: Path loss models for low-height mobiles in forest and urban. Wirel. Pers. Commun. **92**(2), 455–465 (2017)
12. Boban, M.; Barros, J.; Tonguz, O.K.: Geometry-based vehicle-to-vehicle channel modeling for large-scale simulation. IEEE Trans. Veh. Technol. **63**(9), 4146–4164 (2014)
13. Cheng, L.; Henty, B.E.; Stancil, D.D.; Bai, F.; Mudalige, P.: Mobile vehicle-to-vehicle narrow-band channel measurement and characterization of the 5.9 GHz dedicated Short Range Communication (DSRC) frequency band. IEEE J. Sel. Areas Commun. **25**(8), 1501–1516 (2007)
14. Kihei, B.; Copeland, J.A.; Chang, Y.: Improved 5.9 GHz V2V short range path loss model. In: Proceedings - 2015 IEEE 12th International Conference on Mobile Ad Hoc and Sensor Systems, MASS 2015, pp. 244–252, (2015)
15. Cheng, L.; Henty, B.; Stanci, D. D.; Bai, F.; Mudalige, P.: A fully mobile, GPS enabled, vehicle-to-vehicle measurement platform for characterization of the 5.9 GHz DSRC channel. In: IEEE Antennas and Propagation Society, AP-S International Symposium (Digest), pp. 2005–2008, (2007)
16. Andrés, B.B.-C.; Campuzano, J.; Fernández, H.; Balaguer, D.; Vila, A.; Vicent, A.V.-N.; Rodrigo-Peñarrocha, M.; Reig, J.; Rubio, L.: Vehicular-to-vehicular channel characterization and measurement results. Waves **4**, 15–24 (2012)

17. Ibdah, Y.; Ding, Y.: Mobile-to-mobile channel measurements at 1.85 GHz in suburban environments. IEEE Trans. Commun. **63**(2), 466–475 (2015)
18. Miucic, R.; Popovic, Z.; Mahmud, S.M.: Experimental characterization of DSRC signal strength drops. In: IEEE conference on intelligent transportation systems, Proceedings, ITSC, pp. 311–315, (2009)
19. Schumacher, H.; Tchouankem, H.: Highway propagation modeling in VANETS and its impact on performance evaluation. in: 2013 10th Annual Conference on Wireless On-Demand Network Systems and Services, WONS 2013, pp. 178–185, (2013)
20. Nilsson, M.G.; Gustafson, C.; Abbas, T.; Tufvesson, F.: A measurement-based multilink shadowing model for V2V network simulations of highway scenarios. IEEE Trans. Veh. Technol. **66**(10), 8632–8643 (2017)
21. Paier, A.; Karedal, J.; Czink, N.; Dumard, C.; Zemen, T.; Tufvesson, F.; Molisch, A.F.; Mecklenbräuker, C.F.: Characterization of vehicle-to-vehicle radio channels from measurements at 5.2 GHz. Wireless Pers. Commun. **50**(1), 19–32 (2009)
22. Vlastaras, D., Abbas, T., Nilsson, M., Whiton, R., Olback, M., Tufvesson, F.: Impact of a truck as an obstacle on vehicle-to-vehicle communications in rural and highway scenarios. In: 2014 IEEE 6th International Symposium on Wireless Vehicular Communications, WiVeC 2014 - Proceedings, (2014)
23. Stancil, D.; Cheng, L.; Henty, B.; Bai, F.: Highway and rural propagation channel modeling for vehicle-to-vehicle communications at 5.9 GHz. In: 2008 IEEE International Symposium on Antennas and Propagation and USNC/URSI National Radio Science Meeting, APSURSI (2008), vol. **15213**, no. 1, pp. 25–28, (2008)
24. Kuzulugil, K.; Hasirci, Z.; Cavdar, I.H.: Optimum reference distance based path loss exponent determination for vehicle-to-vehicle communication. Turk. J. Electr. Eng. Comput. Sci. **28**(5), 2956–2967 (2020)
25. He, R.; Molisch, A.F.; Tufvesson, F.; Zhong, Z.; Ai, B.; Zhang, T.: Vehicle-to-vehicle propagation models with large vehicle obstructions. IEEE Trans. Intell. Transp. Syst. **15**(5), 2237–2248 (2014)
26. Abbas, T.; Karedal, J.; Tufvesson, F.: Measurement-based analysis: the effect of complementary antennas and diversity on vehicle-to-vehicle communication. IEEE Antennas Wirel. Propag. Lett. **12**, 309–312 (2013)
27. Jiang, S.; Wang, W.; Rashdan, I.: V2V channel modeling at 5.2 GHz for highway environment. China Commun. **19**(11), 112–128 (2022)
28. Sadovaya, Y.; Solomitckii, D.; Mao, W.; Orhan, O.; Nikopour, H.; Talwar, S.; Andreev, S.; Koucheryavy, Y.: Ray-based modeling of directional millimeter-wave V2V transmissions in highway scenarios. IEEE Access **8**, 54482–54493 (2020)
29. Turan, B.; Uyrus, A.; Koc, O. N.; Kar, E.; Coleri, S.: Machine learning aided path loss estimator and jammer detector for heterogeneous vehicular networks. In: 2021 IEEE Global Communications Conference, GLOBECOM 2021 - Proceedings, (2021)
30. Jia, A.; Jiang, S.; Lv, Y.; Zhang, X.; Chang, T.; Rashdan, I.; Unterhuber, P.; Wang, W.: Connectivity analysis of V2V channel at intersections. In: 15th European Conference on Antennas and Propagation, EuCAP 2021, (2021)
31. Xiong, L.; Yao, Z.; Miao, H.; Ai, B.: Vehicle-to-vehicle channel characterization based on ray-tracing for urban road scenarios. Wirel. Commun. Mobile Comput. **2021**, 1–15 (2021)
32. Rappaport, T.S.; et al.: Wireless Communications: Principles and Practice. Prentice hall PTR, New Jersey (1996)
33. Akaike, H.: A new look at the statistical model identification. IEEE Trans. Autom. Control **19**(6), 716–723 (1974)